

Solid-State Kinetic Parameters and Mechanism for the Deaquation-Anation of *trans*-Fluoroaquis(diamine)chromium(III) Complexes Containing Chloride, Bromide, Iodide, and Dithionate. Influence of Amine Size, Entering Anion, and Trans to Cis Isomerization

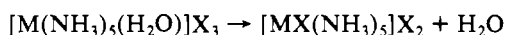
Montserrat Corbella and Joan Ribas*

Received July 19, 1985

The solid-state kinetic parameters for the dehydration-anation of *trans*-[CrF(aa)₂(H₂O)]X₂ (with aa = ethylenediamine (en), 1,3-diaminopropane (tn), 1,2-diaminocyclohexane (chxn); X = Cl, Br, I, ¹/₂ S₂O₆) have been studied by thermogravimetric measurements under both isothermal and nonisothermal conditions. All the complexes, especially the new *trans*-[CrF(chxn)₂(H₂O)]X₂, have been characterized by chemical analysis, electronic and IR spectra, DSC and TG runs, and conductivity measurements. Heating at controlled temperature and time indicated that *trans*-[CrF(en)₂(H₂O)]X₂ and *trans*-[CrF(chxn)₂(H₂O)]X₂ produce *cis*-[CrF(X)(en)₂]X and *cis*-[CrF(X)(chxn)₂]X, respectively. In contrast, *trans*-[CrF(tn)₂(H₂O)]X₂ gives *trans*-[CrF(X)(tn)₂]X in the majority of cases. All the dehydrated complexes have been also characterized as the starting compounds. The activation energy parameters indicate different trends: (a) The gradation in the order I > S₂O₆ > Br > Cl agrees with a dissociative mechanism (S_N1) controlled by the cation/anion ratio. (b) In the chxn complexes, the trans to cis isomerization is independent and quasi-simultaneous with the dehydration-anation process. The mechanism is expected to be via the rupture of one of the Cr^{III}-N(chxn) bonds. (c) This loss of one end of the chelated chxn is constitutive for the intermediate species and, moreover, creates more volume occupied in the lattice when the activated species is formed. As a result of (b) and (c), the E_a value must be greater in the *trans*-[CrF(chxn)₂(H₂O)]X₂ series. Effectively, this is the order found: chxn > en > tn.

Introduction

In the literature there are a great number of papers that support the existence of the so-called "anion effect" in certain reactions in the solid state involving coordination compounds.^{1,2} This effect has been observed, for example, in the reactions of the type



where M = Cr(III), Co(III), Rh(III), Ir(III), Ru(III), and X = Cl, Br, I, SCN, etc., which exhibit different activation energies depending on the nature of X.¹

After the important studies of House¹ and LeMay³ on this subject, these processes can be interpreted in terms of the formation of a nonionic Frenkel defect. That is, the reaction under consideration begins with the loss of a water molecule that must be placed in an interstitial position in the lattice. Creation of this type of defect is equivalent to the initiation of an S_N1 process. The ligand water causing the defect must now diffuse through the lattice. Although the process may be S_N1, there will be a difference in the diffusion coefficient of a Frenkel defect through the lattice depending on the relative size of the ions. Consequently, E_a may vary with the nature of the entering anion.

If we suppose an S_N2 mechanism, this process would require that an anion leave a lattice site and migrate to the complex ion to form a transition state having a coordination number of 7. This is a formation of an ionic Schottky defect, which requires considerable energy.⁴ For these reasons, LeMay³ suggests, for instance, that previous assignments of an S_N2 associative-type mechanism based on the variation of activation parameters (anion effect) are unwarranted.

In this paper we give the results obtained by isothermal and nonisothermal measurements on the complexes *trans*-[CrF(aa)₂(H₂O)]X₂ (aa = ethylenediamine (en), 1,3-diaminopropane (tn), 1,2-diaminocyclohexane (chxn); X = Cl, Br, I, S₂O₆). We have chosen these complexes for three reasons: (a) to study once more the influence of a change of the anion in the calculation of the kinetic parameters; (b) to see the influence of the change of the ligands in the magnitude of the kinetic parameters; (c) to study the influence of trans to cis isomerization that occurs in some of the anation processes, taking into account the intimate relation between the isomerization and the formation of the penta-coordinate species, assuming an S_N1 mechanism.

According to the results presented in this paper, we propose that these dehydration-anation reactions behave, effectively, as

dissociative (D) with the free space in the lattice being an important and determinant factor. The gradation of the activation energy in the order I > S₂O₆ > Br > Cl indicates this dissociative mechanism; the gradation in the order chxn > en > tn indicates that the free space follows the inverse order.

Experimental Section

Preparation of the Compounds. The ethylenediamine (en) and 1,3-diaminopropane (tn) complexes have been prepared according to the methods indicated in the literature: *trans*-[CrF(en)₂(H₂O)]X₂ (X = ClO₄, Cl, Br, I, S₂O₆);^{5,6} *trans*-[CrF(tn)₂(H₂O)]X₂ (X = ClO₄, Cl, Br, I, S₂O₆).^{6,7}

The new complexes have been synthesized as follows:

***trans*-[CrF(chxn)₂(H₂O)](ClO₄)₂.** This compound has been prepared by a method similar to that published in the literature for the ethylenediamine and 1,3-diaminopropane analogues.^{5,7} Anal. Calcd: C, 27.93; H, 5.86; N, 10.86. Found: C, 28.5; H, 5.9; N, 11.0.

***trans*-[CrF(chxn)₂(H₂O)]Cl₂.** A 1.0-g (0.002-mol) amount of *trans*-[CrF(chxn)₂(H₂O)](ClO₄)₂ was dissolved in the minimum amount of concentrated hydrochloric acid, and the solution was cooled in an ice bath to 5 °C. Acetone was added to the solution, and pink crystals of the new product precipitated. These crystals were collected by filtration, washed with acetone, and allowed to dry in air. Anal. Calcd for [CrF(chxn)₂(H₂O)]Cl₂·0.5H₂O: C, 36.31; H, 7.87; N, 14.11; Cl, 17.86. Found: C, 35.9; H, 7.8; N, 14.1; Cl, 17.9.

***trans*-[CrF(chxn)₂(H₂O)]Br₂.** An aqueous solution of *trans*-[CrF(chxn)₂(H₂O)](ClO₄)₂ was treated with an excess of concentrated hydrobromic acid, and the solution was cooled in an ice bath. In a very short time, pink crystals precipitated. The crystals were collected by filtration, washed with acetone, and ether. Anal. Calcd for [CrF(chxn)₂(H₂O)]Br₂: C, 30.20; H, 6.29; N, 11.79; Br, 33.55. Found: C, 30.5; H, 6.5; N, 11.8; Br, 33.6.

***trans*-[CrF(chxn)₂(H₂O)]I₂.** An aqueous solution of *trans*-[CrF(chxn)₂(H₂O)](ClO₄)₂ was treated with an excess of concentrated hydriodic acid, and the solution was cooled in an ice bath. In a very short time, pink-orange crystals precipitated. These crystals were collected by

- (1) House, J. E. *Thermochim. Acta* 1980, 38, 59 and references therein.
- (2) (a) Corbella, M.; Serra, M.; Martinez, M. L.; Ribas, J. *Thermochim. Acta* 1982, 57, 283. (b) Serra, M.; Escuer, A.; Baró, M. D.; Ribas, J. *Ibid.* 1982, 56, 183. (c) Serra, M.; Escuer, A.; Ribas, J. *Ibid.* 1983, 64, 237. (d) Ribas, J.; Serra, M.; Escuer, A.; *Inorg. Chem.* 1984, 23, 2236. (e) Ribas, J.; Escuer, A.; Monfort, M. *Inorg. Chem.* 1985, 24, 1874. (f) Ribas, J.; Monfort, M. *Thermochim. Acta* 1985, 91, 115.
- (3) LeMay, H. E.; Babich, M. W. *Thermochim. Acta* 1981, 48, 147.
- (4) Schmalzreid, H. *Solid State Reactions*; Verlag Chemie: New York, 1974; p 23.
- (5) (a) Vaughn, J. W.; Stvan, O. J.; Magnusson, V. E. *Inorg. Chem.* 1968, 7, 736. (b) Vaughn, J. W. *Synth. React. Inorg. Met.-Org. Chem.* 1979, 6, 685. (c) Vaughn, J. W. *Coord. Chem. Rev.* 1981, 39, 265.
- (6) Ribas, J.; Casabó, J.; Baró, M. D. *Thermochim. Acta* 1981, 47, 271.
- (7) Vaughn, J. W. *Inorg. Nucl. Chem. Lett.* 1968, 4, 183. See also ref 5b.c.

* Author to whom all correspondence should be addressed.

Table I. Electronic Spectra and Conductivity Measurements (Λ) in Aqueous Solution

	λ_{\max}^a (ϵ^b)				Λ^c	$10^3 C^d$
$trans$ -[CrF ₂ (en) ₂] ⁺	525 (16.3)	466 (21.1)	400 (12.8)	350 (14.5)	106	1.0
$trans$ -[CrF(en) ₂ (H ₂ O)] ²⁺	519 (24.2)	454 (25.6)		371 (31.2)	264	1.0
cis -[CrFCl(en) ₂] ⁺		519 (54.2)		385 (36.5)	143	1.44
cis -[CrFBr(en) ₂] ⁺		512 (62.0)		380 (37.7)	190	1.5
cis -[CrFI(en) ₂] ⁺		527 (20.9)		388 (14.6)	148	1.1
cis -[CrF(en) ₂ (S ₂ O ₆)]		529 (45.7)		390 (36.7)	136	0.42
$trans$ -[CrF ₂ (tn) ₂] ⁺	542 (16.5)	462 (20.9)	397 (16.8)	360 (16.4)	102	1.3
$trans$ -[CrF(tn) ₂ (H ₂ O)] ²⁺	533 (20.9)	460 (22.4)		375 (37.8)	253	1.5
$trans$ -[CrFCl(tn) ₂] ⁺	570 (21.9)	460 (24.9)		389 (38.6)	142	1.8
$trans$ -[CrFBr(tn) ₂] ⁺	552 (19.3)	460 (23.2)		382 (14.2)	172	1.4
cis -[CrFI(tn) ₂] ⁺		537 (26.4)		397 (14.2)	180	1.2
cis -/ $trans$ -[CrF(tn) ₂ (S ₂ O ₆)]	510 (28.3)	465 (sh)		375 (31.0)	173	0.9
$trans$ -[CrF ₂ (chxn) ₂] ⁺	529 (19.7)	466 (27.1)	397 (18.8)	354 (21.7)	95	1.6
$trans$ -[CrF(chxn) ₂ (H ₂ O)] ²⁺	520 (25.8)	460 (28.6)		373 (35.4)	213	1.4
cis -[CrFCl(chxn) ₂] ⁺		518 (46.3)		386 (41.7)	184	0.9
cis -[CrFBr(chxn) ₂] ⁺		510 (52.4)		376 (30.3)	190	0.8
cis -[CrFI(chxn) ₂] ⁺		505 (23.3)		358 (18.7)	167	1.6
cis -[CrF(chxn) ₂ (S ₂ O ₆)]		503 (51.8)		376 (37.3)	161	1.1

^a Wavelength in nm. ^b Molar absorptivities in M⁻¹ cm⁻¹. ^c Calculated from resistance measurements of the complex at room temperature; units are cm² Ω^{-1} M⁻¹. ^d Concentration in M.

filtration and washed with acetone and ether. Anal. Calcd for [CrF(chxn)₂(H₂O)]I₂: C, 25.21; N, 9.80; H, 5.25; I, 44.46. Found: C, 25.7; N, 9.9; H, 5.4; I, 43.7.

$trans$ -[CrF(chxn)₂(H₂O)]S₂O₆. A 0.4-g sample of $trans$ -[CrF(chxn)₂(H₂O)](ClO₄)₂ was dissolved in the minimum amount of water, and the solution was cooled in an ice bath. A saturated solution of Na₂S₂O₆·2H₂O was added (0.25 g), and pink crystals of $trans$ -[CrF(chxn)₂(H₂O)]S₂O₆ rapidly precipitated. The crystals were collected as mentioned above. Anal. Calcd for [CrF(chxn)₂(H₂O)]S₂O₆: C, 29.09; H, 6.46; N, 11.32. Found: C, 28.1; H, 6.4; N, 11.3.

cis -[CrCIF(chxn)₂]Cl. A weighed sample of $trans$ -[CrF(chxn)₂(H₂O)]Cl₂ was heated at 200 °C for 1 h. During this time the complex turned from light pink to purple and this was accompanied by a 6.2% loss in weight. This complex appears to be very hygroscopic when exposed to the air for short periods of time. Anal. Calcd for [CrFCl(chxn)₂]-Cl·H₂O: C, 36.31; H, 7.87; N, 14.11. Found: C, 36.9; H, 8.0; N, 14.1.

cis -[CrBrF(chxn)₂]Br. A weighed sample of $trans$ -[CrF(chxn)₂(H₂O)]Br₂ was heated at 200 °C for 1 h. During this time the complex turned from light pink to purple and this was accomplished by a 3.8% loss in weight. This complex, as for the chloride analogue, appeared to be hygroscopic when exposed to the air for short periods of time. Anal. Calcd for [CrBrF(chxn)₂]Br·H₂O: C, 29.10; H, 6.47; N, 11.32. Found: C, 29.2; H, 6.5; N, 11.2.

cis -[CrFI(chxn)₂]I. A weighed sample of $trans$ -[CrF(chxn)₂(H₂O)]I₂ was heated at 200 °C for 1 h. During this time the complex turned from orange to reddish purple. This color change was accompanied by a 3.15% loss in weight. Anal. Calcd for [CrFI(chxn)₂]I: C, 25.25; H, 5.30; N, 9.81. Found: C, 25.4; H, 5.4; N, 9.7.

cis -[CrF(S₂O₆)(chxn)₂]. A weighed sample of $trans$ -[CrF(chxn)₂(H₂O)]S₂O₆ was heated at 180 °C for 10 min. During this time the complex turned from light pink to purple and this was accompanied by a 3.77% loss in weight. Anal. Calcd for [CrF(S₂O₆)(chxn)₂]: C, 31.40; N, 12.21; H, 6.15. Found: C, 31.5; N, 12.1; H, 6.3.

Techniques. Infrared spectra were recorded on a Beckman IR 20 A spectrophotometer purged with dry air. Samples were prepared by using the KBr technique. Electronic absorption spectra were recorded in solution and in the solid phase (KBr disk or diffuse reflectance) on a Beckman 5230 UV spectrophotometer. Thermogravimetric analyses were carried out on a Perkin-Elmer Model TGS-1 system, under nitrogen (10 cm³ min⁻¹), the sample size being in the range 4–7 mg. The heating rate for nonisothermal experiments was 5 °C/min. To resolve the nonisothermal TG curves, we used the widely employed approximation of Coats and Redfern.⁸ All calculations were made with a FORTRAN IV program. Conductivity measurements were carried out with a Radiometer CDM-3 conductivity bridge. X-ray powder diffractions were recorded on a Philips PW-1030 diffractometer, with graphite-monochromatized Cu K α radiation.

Results

(a) Characterization of the New Compounds. All the compounds were characterized by analytical data (see Experimental Section), DSC and TG measurements, electronic and IR spectra,

and molar conductivity measurements at room temperature.

(1) Molar Conductivity Measurements. In Table I are shown the values of the molar conductivity measurements at room temperature for all the compounds described in this work (in the series $trans$ -[CrF(aa)₂(H₂O)]²⁺ only the conductivity for the more soluble salt was measured). The compounds of the series $trans$ -[CrF(aa)₂(H₂O)]²⁺ have molar conductivity indicating three ions (200–250 Ω^{-1} cm² mol⁻¹). In contrast, the $trans$ - and cis -[CrFX(aa)₂]X have a conductivity nearly that of two ions, but greater than expected. This increase is due to the aquation of the [CrFX(aa)₂]⁺ cation. According to the data shown in Table I, the variation of the conductivity indicates that the aquation is greater for the Br and I ligands, and lower for the chloro compounds, in accordance with the literature data.⁵ The values of the iodo compounds are lower than those of the bromo complexes, due to the lower mobility of the iodide ion.

(2) Electronic Spectra. The electronic spectra have been very useful in determining the $trans$ or cis character of the new compounds. In the ethylenediamine complexes and in the majority of the tn derivatives, these characteristics have already been studied.^{5,7} Consequently, in these cases, we proceed only to the experimental verification.

The visible electronic spectra of fluoro complexes of chromium(III) which result from spin-allowed transitions can be easily explained in terms of current theory. Thus, one would expect in order of increasing energy the following three spin-allowed transitions: ⁴A_{2g} → ⁴T_{2g}, ⁴A_{2g} → ⁴T_{1g}(F), and ⁴A_{2g} → ⁴T_{1g}(P). Since the third spin-allowed transition is shifted to higher energies due to mixing of the two ⁴T_{1g} excited states, the expected transition is sometimes obscured by another transition that results from electron transfer from the ligand to an acceptor orbital centered on the chromium. Only in the case of CrF₆³⁻ are all three transitions observed.

Moreover, theory predicts that the CrN₄F₂ or CrN₄FX core complexes with two different local site symmetries ($trans$ -D_{4h} and cis -C₂) should exhibit splitting of the excited states with the splitting of the $trans$ complex twice that found for the cis isomer.⁹ In the cases of $trans$ -[CrF₂(aa)₂]⁺ and $trans$ -[CrF(aa)₂(H₂O)]²⁺ such a splitting is observed, whereas the effect is absent in cis -[CrF₂(aa)₂]⁺ and cis -[CrF(aa)₂(H₂O)]²⁺.^{5,7} Table I contains the spectral data for all the fluoro-containing complexes studied in this work.

From the data shown in Table I we can deduce that the starting complexes [CrF(aa)₂(H₂O)]²⁺ are of $trans$ geometry. The assignment of the $trans$ structure is well supported by the visible absorption spectra, which contain the three characteristic bands

(8) Coats, A. W.; Redfern, J. P. *Nature (London)* **1964**, *201*, 68.

(9) Lever, A. B. P. *Inorganic Electronic Spectroscopy*, 2nd ed.; Elsevier: Amsterdam, 1984.

Table II. Representative Peaks of Powder Diffraction of $trans\text{-}[\text{CrF}(\text{aa})_2(\text{H}_2\text{O})]\text{X}_2 \cdot n\text{H}_2\text{O}$

$trans\text{-}[\text{CrF}(\text{en})_2(\text{H}_2\text{O})]\text{X}_2 \cdot n\text{H}_2\text{O}$					
X = Cl ⁻ , n = 0		X = Br ⁻ , n = 0		X = I ⁻ , n = 0	
d	I/I ₀	d	I/I ₀	d	I/I ₀
8.34	75	8.34	45	8.50	40
6.23	20	4.62	30	4.72	50
5.83	35	4.29	100	4.42	100
5.54	25	4.19	15	4.27	50
4.39	30	4.07	20	4.15	80
4.11	100	3.78	40	3.83	95
3.83	30	3.37	20	3.45	35
3.06	25	3.32	35	3.43	50
2.88	25	3.23	25	3.28	30
$trans\text{-}[\text{CrF}(\text{tn})_2(\text{H}_2\text{O})]\text{X}_2 \cdot n\text{H}_2\text{O}$					
X = Cl ⁻ , n = 0.5		X = Br ⁻ , n = 0.5		X = I ⁻ , n = 1	
d	I/I ₀	d	I/I ₀	d	I/I ₀
8.19	100	8.34	100	7.62	30
6.51	10	6.60	5	5.40	50
3.93	25	4.00	85	4.19	100
3.37	15	3.43	40	4.13	35
3.25	35	3.28	60	3.32	15
3.04	40	3.08	90	2.84	45
2.90	15	2.94	40	2.80	40
2.44	20	2.48	50	2.51	15
$trans\text{-}[\text{CrF}(\text{chxn})_2(\text{H}_2\text{O})]\text{X}_2 \cdot n\text{H}_2\text{O}$					
X = Cl ⁻ , n = 0.5		X = Br ⁻ , n = 0		X = I ⁻ , n = 0	
d	I/I ₀	d	I/I ₀	d	I/I ₀
5.79	95	4.57	30	4.62	35
4.23	100	4.44	50	4.46	50
3.80	90	4.07	25	4.11	30
2.98	20	3.97	25	3.98	30
2.49	15	3.80	100	3.82	100
2.34	15	3.18	20	3.21	20
2.13	15	3.02	25	3.02	25

for this kind of compound. Such a configuration has been recently confirmed by X-ray structural determination of several salts of $trans\text{-}[\text{CrF}(\text{en})_2(\text{H}_2\text{O})]^{2+}$ and $trans\text{-}[\text{CrF}(\text{tn})_2(\text{H}_2\text{O})]^{2+}$.¹⁰ The total agreement of the bands of the 1,2-cyclohexanediamine analogues permit us to assign the trans geometry in these complexes.

The chloro, bromo, iodo, and dithionate derivatives, when dehydrated, present different characteristics if they are ethylenediamine, 1,3-diaminopropane, or 1,2-diaminocyclohexane compounds. With the en and chxn amines we observe in the visible spectrum two symmetrical and well-defined bands. These features clearly indicate the cis configuration. In contrast, with the tn ligand the behavior is different. The visible spectra of the chloro and bromo derivatives present the three characteristic bands of the trans configuration. With the dithionate ligand the visible spectrum corresponds to a mixture of trans and cis configurations, and with the iodo ligand and dominant species is the cis configuration. This lower tendency toward isomerization in the 1,3-diaminopropane complexes has already been reported in this same series, $trans\text{-}[\text{CrF}(\text{tn})_2(\text{H}_2\text{O})]^{2+}$, by Vaughn and co-workers.⁷ They report that only with the SCN⁻ anion is there trans-cis isomerization. In the series $trans\text{-}[\text{CrX}_2(\text{aa})_2]\text{X}$, Tsuchiya and Uehara corroborate this feature.¹¹ The trans-cis isomerization was identified only in the bis(amine) complexes containing en, tn, and chxn that can form five-membered chelated rings with

Table III. Temperature Interval (ΔT) for DSC and TG Diagrams^a

	ΔT		ΔH	final product
	DSC	TG		
$trans\text{-}[\text{CrF}_2(\text{en})_2]\text{Cl}$	50–250			trans
$trans\text{-}[\text{CrF}_2(\text{tn})_2]\text{Cl}$	120–185		30.4	trans
$trans\text{-}[\text{CrF}_2(\text{chxn})_2]\text{Cl}$	160–230		55.5	cis
$trans\text{-}[\text{CrF}(\text{en})_2(\text{H}_2\text{O})]\text{Cl}_2$	112–180	60–180	51.2	cis
$trans\text{-}[\text{CrF}(\text{en})_2(\text{H}_2\text{O})]\text{Br}_2$	130–200	110–190	71.7	cis
$trans\text{-}[\text{CrF}(\text{en})_2(\text{H}_2\text{O})]\text{I}_2$	175–210	140–200	37.3	cis
$trans\text{-}[\text{CrF}(\text{en})_2(\text{H}_2\text{O})]\text{S}_2\text{O}_6$	142–195	100–160	42.2	cis
$trans\text{-}[\text{CrF}(\text{tn})_2(\text{H}_2\text{O})]\text{Cl}_2$	85–115	85–100	61.6	trans
$trans\text{-}[\text{CrF}(\text{tn})_2(\text{H}_2\text{O})]\text{Br}_2$	75–120	85–100	68.7	trans
$trans\text{-}[\text{CrF}(\text{tn})_2(\text{H}_2\text{O})]\text{I}_2$	120–160	110–150	47.1	cis
$trans\text{-}[\text{CrF}(\text{tn})_2(\text{H}_2\text{O})]\text{S}_2\text{O}_6$	160–200	160–185	41.6	trans + cis
$trans\text{-}[\text{CrF}(\text{chxn})_2(\text{H}_2\text{O})]\text{Cl}_2$	120–240	80–220	53.9	cis
$trans\text{-}[\text{CrF}(\text{chxn})_2(\text{H}_2\text{O})]\text{Br}_2$	150–240	120–220	80.7	cis
$trans\text{-}[\text{CrF}(\text{chxn})_2(\text{H}_2\text{O})]\text{I}_2$	125–230	80–235	85.5	cis
$trans\text{-}[\text{CrF}(\text{chxn})_2(\text{H}_2\text{O})]\text{S}_2\text{O}_6$	145–220	150–200	82.1	cis

^a ΔT is in °C. ΔH (in kJ/mol) was obtained from DSC diagrams, and the geometry of the final product was obtained by both methods (DSC and TG; The water of crystallization had been previously eliminated).

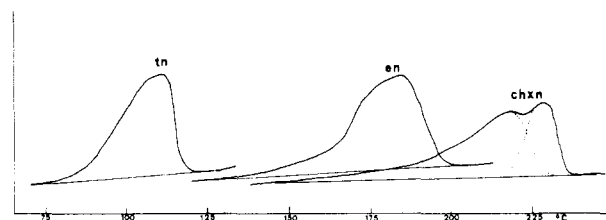


Figure 1. DSC diagrams for the dehydration-anation of $trans\text{-}[\text{CrF}(\text{aa})_2(\text{H}_2\text{O})]\text{Br}_2$ (aa = en, tn, chxn). The peaks are endothermic. The DSC diagrams for chloride, iodide, and dithionate salts are very similar, especially in the en and tn series; in the chxn series the bromide is the unique salt, which presents two well-defined peaks. (See Table II for temperature intervals and ΔH values for each reaction.)

metal ions, whereas cis-trans isomerization was detected in the simple bis(diamine) complexes containing tn that form six-membered rings. Consequently, we cannot expect that the trans-cis isomerization occurs easily in the tn derivatives. From the data shown in Table I we can also deduce the high tendency for the aquation with the ligands Br and I to give the species $cis\text{-}[\text{CrF}(\text{aa})_2(\text{H}_2\text{O})]^{2+}$, in agreement with the literature data.⁵ This fact is in accord with the measurements of molar conductivity reported above.

(3) X-ray Powder Diffraction. The obtained results (Table II) indicate isomorphism in the tn and chxn series when the numbers of water molecules of crystallization are the same; in the en series all the complexes are obtained without water molecules of crystallization but only the Br⁻ and I⁻ complexes are isomorphous.

(b) DSC Measurements. We have recorded all the DSC diagrams for the corresponding dehydration-anation reactions in order to calculate ΔH for these reactions and compare with the parameters derived from the TG measurements (see below) and to see the possibility of separating the isomerization and dehydration in the en and chxn compounds. When the complexes had water of crystallization, two perfectly defined peaks were observed: the first corresponding to the loss of water of crystallization and the second to the dehydration-anation reaction.

The temperature intervals for the anation reactions, ΔH for the reactions, and the geometries of the final product are given in Table III.

In Figure 1 several representative DSC diagrams are presented (the others are very similar in each series). The DSC diagrams for the en and tn series are very defined with rather small temperature intervals. In contrast, the DSC diagrams for the chxn complexes are less defined and less symmetrical and the interval temperatures are very great.

For example, in $trans\text{-}[\text{CrF}(\text{chxn})_2(\text{H}_2\text{O})]\text{Br}_2$ (Figure 1) one endothermic peak is observed, clearly split into two components.

(10) Solans, X.; Font Altaba, M.; Monfort, M.; Ribas, J. *Acta Crystallogr., Sect. B: Struct. Crystallogr. Cryst. Chem.* **1982**, *2899*. (b) Solans, X.; Font Altaba, M.; Casabó, J.; Ribas, J. *Cryst. Struct. Commun.* **1982**, *11*, 1199.

(11) (a) Tsuchiya, R.; Uehara, A. *Thermochim. Acta* **1981**, *50*, 93. (b) Uehara, A.; Nishiyama, Y.; Tsuchiya, R. *Inorg. Chem.* **1982**, *21*, 2422.

Table IV. Computed Kinetic Parameters for $\text{trans-}[\text{CrF}(\text{chxn})_2(\text{H}_2\text{O})]\text{Br}_2$ from the Equations for Growth, Nucleation–Growth, and Nucleation Mechanisms

	growth model			nucleation–growth (Avrami-Erofeev law)		nucleation model (power law)		
	$n = 0$	$n = 0.4$	$n = 0.8$	$n = 1$	$n = 2$	$n = 0.2$	$n = 0.3$	$n = 0.4$
Nonisothermal Measurements								
E_a , kJ mol ⁻¹	36.95	42.75	49.18	52.63	22.58	214.62	140.59	103.57
r^2	0.9996	0.9970	0.9922	0.9892	0.9859	0.9996	0.9996	0.9996
K_0	3.4×10^2	2.1×10^3	1.5×10^4	4.3×10^4	5	2.3×10^{22}	1.7×10^{14}	1.3×10^{10}
Isothermal Measurements								
E_a , kJ mol ⁻¹	151.59	148.18	144.85	143.22	148.55	130.79	137.41	141.70
r^2	0.9983	0.9987	0.9990	0.9992	0.9987	1.0000	0.9996	0.9992
K_0	3.6×10^{13}	2.2×10^{13}	1.4×10^{13}	1.1×10^{13}	2.2×10^{13}	1.3×10^{11}	1.0×10^{12}	3.3×10^{12}

The first corresponds to the isomerization process and the second to the anation process, according to the spectroscopic measurements. The ΔH value calculated for the first peak corresponds, almost exactly, to the ΔH value for the isomerization of $\text{trans-}[\text{CrF}_2(\text{chxn})_2]\text{Cl}$ (Table III). In order to best understand this phenomenon, the DSC diagrams for $\text{trans-}[\text{CrF}_2(\text{aa})_2]\text{Cl}$ (without the possibility of dehydration–anation) were recorded. The chxn complex presents a very asymmetrical peak, starting at 160 °C and finishing at 230 °C. The final product is the *cis-}[\text{CrF}_2(\text{chxn})_2]\text{Cl} isomer. Consequently, there has been an isomerization process. For $\text{trans-}[\text{CrF}_2(\text{en})_2]\text{Cl}$ between 50 and 250 °C there is no observable peak in the DSC diagram; obviously, the final product is the same as the starting $\text{trans-}[\text{CrF}_2(\text{en})_2]\text{Cl}$. For $\text{trans-}[\text{CrF}_2(\text{tn})_2]\text{Cl}$ there is a small endothermic peak (Table III), but the final product is the same $\text{trans-}[\text{CrF}_2(\text{tn})_2]\text{Cl}$ without isomerization.*

Consequently, if we compare the behavior of the $\text{trans-}[\text{CrF}_2(\text{aa})_2]\text{Cl}$ series with that of the $\text{trans-}[\text{CrF}(\text{aa})_2(\text{H}_2\text{O})]\text{X}_2$ series, we observe that in the tn complexes the isomerization is almost never produced; in the en complexes the isomerization is produced only when there is a dehydration–anation process and, in contrast, in the chxn series such an isomerization is independent of the dehydration–anation.

(c) TG Measurements. Calculation of Kinetic Parameters. In order to determine the kinetic parameters, we have registered one nonisothermal TG run for all the studied substances. Without water of crystallization being taken into account, the temperature intervals for the dehydration–anation reactions are given in Table III (compared with the DSC intervals for the same reaction). Also in Table III are indicated the new species formed, characterization by analysis and spectroscopic measurements. In all these cases the analytical data are in agreement with the formulas proposed and the electronic spectra clearly indicate the trans or cis geometry. From Table II we can qualitatively deduce that the tendency to the dehydration–anation follows the order $\text{Cl} > \text{Br} > \text{I}$, with the dithionate being an intermediate case. Such a result agrees with the coordinative capacity of these ligands.

From nonisothermal TG runs we selected several temperatures in the anation interval to carry out the isothermal TG runs necessary to calculate the kinetic parameters. The final products of the isothermal TG studies were also analyzed and studied by electronic spectroscopy to determine whether the geometry is trans or cis.

The kinetic parameters were determined on the basis of the general kinetic relation^{12,13}

$$d\alpha/dt = f(\alpha) k(T)$$

or

$$\int_0^1 d\alpha/f(\alpha) = \int_{T_1}^{T_2} k(T) dt = g(\alpha)$$

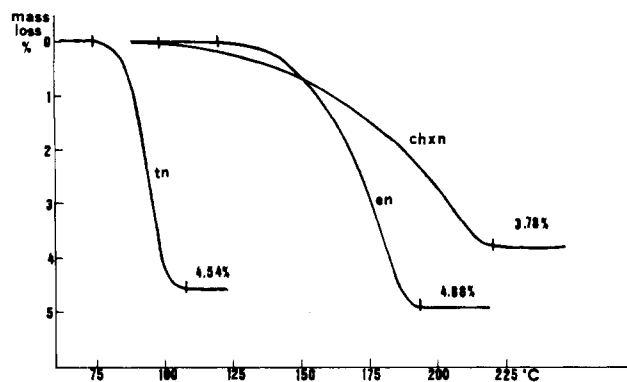


Figure 2. Representative nonisothermal TG diagrams for the dehydration–anation of $\text{trans-}[\text{CrF}(\text{aa})_2(\text{H}_2\text{O})]\text{Br}_2$ ($\text{aa} = \text{en}, \text{tn}, \text{chxn}$). The TG runs for the other salts are very similar. (See Table II for temperature intervals.)

where α is the fraction decomposed and $k(T)$ follows the Arrhenius law ($k(T) = K_0 \exp(-E_a/RT)$), with K_0 being the frequency factor and E_a the activation energy. The expression $g(\alpha)$ depends on the mechanism of the solid-state reaction: diffusion, nucleation, growth, or nucleation–growth.¹⁴ Each process can be studied with use of several expressions of $g(\alpha)$ depending on α and n (the reaction order).

Kinetic parameters are very difficult to calculate by only nonisothermal TG curves¹⁴ due to ignorance of the true $g(\alpha)$ expression. It is necessary to compare the results obtained by nonisothermal and isothermal TG measurements for all the $g(\alpha)$ expressions in order to calculate the true activation energy and to know the physical mechanism of the solid-state process. For this reason we have recorded not only the nonisothermal TG curves (Figure 2) for each compound but also the isothermal TG curves at several different temperatures for each compound.

In both methods (nonisothermal and isothermal) all the principal expressions of $g(\alpha)$ reported in the literature¹⁴ have been used. The computation for each $g(\alpha)$ value and for each n value has been carried out with an ad hoc FORTRAN IV program.

The physical mechanism is assigned and the corresponding kinetic parameters are calculated on the basis of agreement in the activation energy, frequency factor, and r^2 (regression coefficient) values in both nonisothermal and isothermal methods. As found in the literature,^{1–3} the solid-state deaquation–anation reactions of $[\text{M}(\text{NH}_3)_5(\text{H}_2\text{O})]^{3+}$ and similar cations behave according to growth, nucleation, or nucleation–growth models. In effect, the values of E_a , K_0 , and r^2 found by us with diffusion models are inconsistent. For this reason, in Table IV only the values found for one compound with the growth, nucleation, and nucleation–growth models are reported. The calculations for the other 11 products are very similar and are not reported here in order not to lengthen the paper. With the possible deviation and

(12) Young, D. A. *Decomposition of Solids*; Pergamon: Oxford, England, 1966; Chapter 1.

(13) Garner, W. E. *The Chemistry of the Solid State*; Butterworths: London, 1955; Chapter 5.

(14) Bamford, D. H., Ed. *Comprehensive Chemical Kinetics*, Elsevier: Amsterdam, 1980; Chapter 3, Vol. 22.

Table V. Average Kinetic Parameters^a

	model; <i>n</i>	log K_0	E_a	r^2	$\Delta S^\ddagger \pm \sigma$	ΔH^\ddagger
<i>trans</i> -[CrF(en) ₂ (H ₂ O)]Cl ₂	power law; 0.6	10.50	107.59	0.9965	-13.17 ± 1.2	103.87
<i>trans</i> -[CrF(en) ₂ (H ₂ O)]Br ₂	power law; 0.65	11.94	125.90	0.9836	-6.75 ± 1	121.90
<i>trans</i> -[CrF(en) ₂ (H ₂ O)]I ₂	growth; 0.4	14.98	151.96	0.9948	15.34 ± 1.2	148.28
<i>trans</i> -[CrF(en) ₂ (H ₂ O)]S ₂ O ₆	Avrami; 1.5	16.09	148.47	0.9979	12.37 ± 0.6	144.80
<i>trans</i> -[CrF(tn) ₂ (H ₂ O)]Cl ₂ ^b	Avrami; 3.5	6.37	60.83	0.9931	-31.73 ± 0.5	57.72
<i>trans</i> -[CrF(tn) ₂ (H ₂ O)]Br ₂	Avrami; 3.5	3.98	44.65	0.9947	-42.69 ± 0.4	41.53
<i>trans</i> -[CrF(tn) ₂ (H ₂ O)]I ₂	Avrami; 3	6.67	69.36	0.9984	-22.41 ± 0.5	66.09
<i>trans</i> -[CrF(tn) ₂ (H ₂ O)]S ₂ O ₆	Avrami; 2.5	10.09	107.45	0.9953	-15.08 ± 0.8	103.65
<i>trans</i> -[CrF(chxn) ₂ (H ₂ O)]Cl ₂	power law; 0.2	11.92	135.50	0.9953	-6.85 ± 1.9	131.40
<i>trans</i> -[CrF(chxn) ₂ (H ₂ O)]Br ₂	power law; 0.3	12.00	137.41	0.9996	-6.60 ± 0.7	133.12
<i>trans</i> -[CrF(chxn) ₂ (H ₂ O)]I ₂	power law; 0.3	20.74	224.18	0.9975	33.35 ± 0.6	219.68
<i>trans</i> -[CrF(chxn) ₂ (H ₂ O)]S ₂ O ₆	power law; 0.5	17.31	171.64	0.9995	17.87 ± 0.7	167.64

^a E_a and ΔH^\ddagger are in kJ/mol, and ΔS is in cal/K·mol. In general the fraction decomposed, α , was between 0.195 and 0.805. The water of crystallization had been previously eliminated. ^b α was between 0.3 and 0.805 due to the difficulty in separating the water of crystallization and coordinated water. For this reason, the E_a value is not accurate.

error of these values taken into account, the final average kinetic parameters calculated are given in Table V.

Discussion

From the results of Table V we find, especially, two aspects: (a) E_a is low, in all the cases; (b) E_a varies with the entering anion and with the ligands.

With regard to (a), and with the CFAE (crystal field activation energy) taken into account, according to the theory of Basolo and Pearson¹⁵ for the homogeneous kinetics, high values of E_a have a better correspondence with an S_N2 mechanism while low values have a better correspondence with S_N1. In our case, in an S_N2 reaction, the formation of a seven-coordinated complex (pentagonal bipyramid), on the basis of a crystal field model, requires $4.26Dq^{15}$ (Dq being about 25 kJ/mol),¹⁶ which alone would be about 100 kJ/mol. If the activated complex were an octahedral wedge, the energy required would be only $1.8Dq$ (nearly 50 kJ/mol, lower than the E_a found). However, considering that in an S_N2 reaction the heptacoordination suggests a Schottky-type defect formation in an ionic crystal, this case requires high energy ($E_{\text{defect}} = 0.24U$; U = lattice energy).⁴

The mechanism, therefore, might be S_N1 (dissociative mechanism) with the formation of a square-base-pyramid activated complex, requiring only $2.00Dq^{15}$ (activation energy about 50 kJ/mol; for a trigonal-bipyramid activated complex the mechanism would require $5.7Dq$).¹⁵ Consequently, the transition state is determined by the water loss and an nonionic Frenkel defect formation, which implies, theoretically, no variation of the activation energy regarding similar entering anions.

With respect to (b), why are the energy values in the three series so different and why in each series do we find a gradation in the E_a values following, in general, the Cl < Br < I order (in the tn series, the E_a value for Cl⁻ is not accurate, due to the difficulty in separating the water of crystallization and coordinated water)? In all the cases, the E_a values for the dithionate compounds are intermediate.

First of all, we must take into consideration that we have to neglect the complete structural factors, since all the attempts to obtain crystals suitable for structural determination failed. The complexes undergo anation and decomposition. The isomorphism of two salts in each series (Table II) indicates that the variation in E_a is not derived from different crystallization systems, since the salts have analogous structures.

We may point out the following possibility: If we suppose a dissociative mechanism, for a given size of cation, diffusion of interstitial defects depends on the size of the anion (so the comparative sizes of anion and cation).^{1,3} This is the so-called

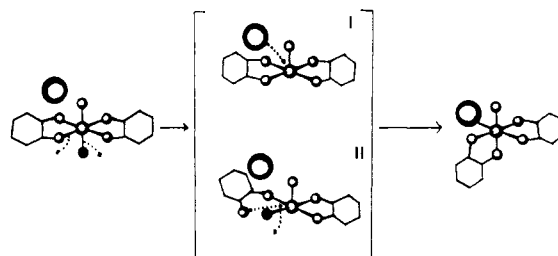


Figure 3. Proposed dissociative mechanism for the dehydration-anation of *trans*-[CrF(chxn)₂(H₂O)]X₂. The intermediate is a square-based pyramid. There is *trans* to *cis* isomerization. This isomerization can be explained as in the ethylenediamine case (Figure 4) (I) or, more accurately, by the rupture of the Cr-N(amine) bond (II) (● = water molecule).

“free-space” theory, elaborated by House and repeatedly found by us in a large series of aqua amine complexes.² In our case, lacking the structural factors, we can only say that, if water is set free from the complex ion in forming the transition state, the escape of a water molecule will be, for instance, easier for the chloride compound (radius 1.81 Å) than for the iodide complex (radius 2.20 Å). Effectively, the radius of the iodide will be similar to the radius of the voluminous cation. Indeed, the packing will possibly be more compact.

The problem that arises is the relation between the E_a values of compounds with different amines (en, tn, chxn). Experimentally we find the following sequence: tn < en < chxn. Why this order?

The DSC studies of *trans*-[CrF₂(aa)₂]Cl compounds aid us in interpreting the order. DSC diagrams showed that only in the chxn case (see above) could there be isomerization. To compare, we sought in the literature similar processes: there is only information about the isomerization reactions of *trans*-[CrX₂(aa)₂]X with X = Cl, Br and aa = en, tn, chxn, reported by Tsuchiya and Uehara,¹¹ as has been indicated in Electronic Spectra. According to these authors it seems clear that in these cases the isomerization behaves via, first, bond rupture of the Cr-N(amine) bond and, second, of the Cr-X(halide) bond.

This Cr-X(halide) bond rupture in the chloro and bromo complexes of chromium(III) is not at all consistent in the case of fluoro complexes (X = F), taking into account the strong character of the Cr(III)-F bond.⁵ Consequently, in the *trans*-[CrF₂(chxn)₂]Cl case the isomerization occurs via the rupture of one Cr-N(amine) bond forming a pentacoordinate species, which passes from *trans* to *cis* geometry by internal rearrangement without Cr-F bond rupture. If this process is extrapolated to the *trans*-[CrF(chxn)₂(H₂O)]²⁺ series, and we suppose that the isomerization and the anation are independent and quasi-simultaneous (we may pose this hypothesis by taking into account the DSC diagrams), the measured E_a value is not only the activation energy of the dehydration-anation process but also the activation energy of the Cr-N(amine) bond rupture (Figure 3). The cases of the en and tn analogues are very different. The

(15) Basolo, F.; Pearson, R. G. *Mechanisms of Inorganic Reactions*, 2nd ed.; Wiley: New York, 1962; Chapter 3.

(16) Huheey, J. E. *Inorganic Chemistry*, 3rd ed.; Harper and Row: London, 1983; p 384.

(17) Solans, X.; Miravittles, C.; Germain, G. *Acta Crystallogr., Sect. B: Struct. Crystallogr. Cryst. Chem.* 1979, B35, 2181.

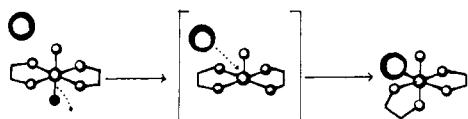


Figure 4. Proposed dissociative mechanism for the dehydration-anation of $trans\text{-}[\text{CrF}(\text{en})_2(\text{H}_2\text{O})]\text{X}_2$. The intermediate is a square-based pyramid; there is no rupture of the Cr-N(amine) bond, and the trans to cis isomerization is due to the entering anion X (● = water molecule).

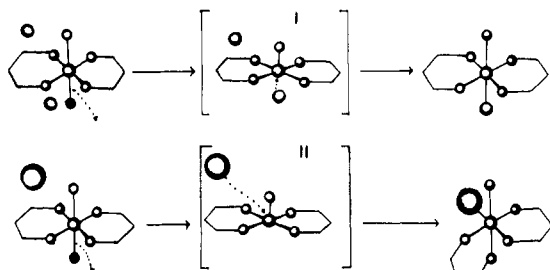


Figure 5. Proposed dissociative mechanism for the dehydration-anation of $trans\text{-}[\text{CrF}(\text{tn})_2(\text{H}_2\text{O})]\text{X}_2$. The intermediate is a square-based pyramid. There is no rupture of the Cr-N(amine) bond. When the entering anion, X^- , is small (Cl, Br), there is no trans to cis isomerization (I); when the entering anion is larger (I, S_2O_6), there is isomerization (II) (● = water molecule).

nonisomerization of the $trans\text{-}[\text{CrF}_2(\text{aa})_2]\text{Cl}$ (aa = en, tn) series indicates that the trans to cis isomerization, in all the $trans\text{-}[\text{CrF}(\text{en})_2(\text{H}_2\text{O})]^{2+}$ salts and in the iodide and dithionate salts of $trans\text{-}[\text{CrF}(\text{tn})_2(\text{H}_2\text{O})]^{2+}$, occurs after and is due to the de-

hydration-anation process. In this case there is no rupture of the $\text{Cr}^{\text{III}}\text{-N}(\text{amine})$ bond.

Conclusions

The lack of X-ray structural data forces us to neglect the structural aspects of the solid-state transformation. Consequently, we are very limited in the interpretation of the results. But, taking into account all the experimental facts, especially the isomorphism, we can point out the following reasonable possibilities:

(a) E_a increases with the size of the anion ($\text{I} > \text{Br} > \text{Cl}$) due to the existence of less free space in the lattice, created by the packing of the anions, which are more or less similar in size with the voluminous $trans\text{-}[\text{CrF}(\text{chxn})_2(\text{H}_2\text{O})]^{2+}$ cation.

(b) E_a varies according to $\text{chxn} > \text{en} > \text{tn}$, possibly due to the different sizes of the amines and the isomerization process that occurs in many cases.

(c) Only in the chxn case may the isomerization be explained by the rupture of the $\text{Cr}^{\text{III}}\text{-N}(\text{amine})$ bond, while in the other two cases, the experimental data indicate one internal rearrangement of the pentacoordinate intermediate without rupture of the Cr-N(amine) bond.

(d) As a result of this, in the chxn case, E_a must correspond to two quasi-simultaneous processes: the dehydration and the Cr-N(amine) bond rupture. In contrast, in the en and tn cases, E_a corresponds only to the dehydration process, without rupture of the Cr-N(amine) bond. Consequently, E_a must be lower in the en and tn cases, compared with that in the chxn compounds. This is the experimental fact.

Contribution from the Paul M. Gross Chemical Laboratory,
Duke University, Durham, North Carolina 27706

Boron Analogues of Choline. 2.¹ Efficient Syntheses of Boron Analogues of Choline, Acetylcholine, and Substituted Acetylcholines

Bernard F. Spielvogel,* Fahim U. Ahmed,[†] and Andrew T. McPhail

Received April 7, 1986

An efficient synthesis of isoelectronic and isostructural boron analogues of acetylcholine [$\text{CH}_3\text{C}(\text{O})\text{OCH}_2\text{CH}_2\text{N}(\text{Me}_2)\text{BH}_3$], benzoylcholine, (phenylacetyl)choline, and (phenoxyacetyl)choline from the reaction of the corresponding ester hydrochlorides with Et_4NBH_4 is described. The ester hydrochlorides are prepared from $\text{Me}_2\text{NCH}_2\text{CH}_2\text{OH}$ and the corresponding acid chlorides. Both reactions are very mild and give almost quantitative yields of products. A boron analogue of choline is similarly prepared from $\text{Me}_2\text{NCH}_2\text{CH}_2\text{OH}\cdot\text{HCl}$, which is in turn made efficiently from dimethylethanolamine and anhydrous HCl. ((Trimethylamine-boryl)carbonyl)choline is prepared by condensing trimethylamine-carboxyborane and the boron analogue of choline with dicyclohexylcarbodiimide. A boron analogue of suberoyldicholine is prepared from the reaction of the corresponding diester hydrochloride with NaBH_4 .

We are interested in the synthesis and characterization of isoelectronic and isostructural boron analogues of biologically important molecules. These may be of use to probe fundamental biochemical events at the molecular level as well as to provide entirely new classes of compounds of potential pharmacological value. Along these lines we have prepared some of the first examples of boron analogues of the α -amino acids²⁻⁴ and their related precursors^{5,6} and derivatives.^{7,8} These analogues, typified by the protonated glycine analogue,² $\text{H}_3\text{N}\cdot\text{BH}_2\text{CO}_2\text{H}$, contain four-coordinate boron and possess appreciable air and hydrolytic stability. They have been found to possess significant pharmacological activity, in particular, antitumor,⁹⁻¹¹ antiarthritic,¹² and hypolipidemic^{13,14} activity in animal model studies.

Boron analogues of other important biologically active molecules such as neurotransmitters can be envisioned. In a previous com-

- (1) A preliminary communication describing the synthesis of **1b** has been published: Spielvogel, B. F.; McPhail, A. T.; Ahmed, F. U. *J. Am. Chem. Soc.* **1986**, *108*, 3824.
- (2) Spielvogel, B. F.; Das, M. K.; McPhail, A. T.; Onan, K. D.; Hall, I. H. *J. Am. Chem. Soc.* **1980**, *102*, 6343.
- (3) Spielvogel, B. F.; Wojnowich, L.; Das, M. K.; McPhail, A. T.; Hargrave, K. D. *J. Am. Chem. Soc.* **1976**, *98*, 5702.
- (4) Spielvogel, B. F. *Boron Chemistry-4*; IUPAC, Inorganic Chemistry Division; Parry, R. W., Kodama, G., Eds.; Pergamon: New York, 1980; pp 119-129.
- (5) Wisian-Neilson, P.; Das, M. K.; Spielvogel, B. F. *Inorg. Chem.* **1978**, *17*, 2327.
- (6) Spielvogel, B. F.; Harchelroad, F., Jr.; Wisian-Neilson, P. *J. Inorg. Nucl. Chem.* **1979**, *41*, 123.
- (7) Spielvogel, B. F.; Ahmed, F. U.; Morse, K. W.; McPhail, A. T. *Inorg. Chem.* **1984**, *23*, 776.

[†] Present address: Research & Development Division, Colgate-Palmolive Co., Piscataway, NJ 08854.